Article

Numerical Solution for Crack Phenomenon in Dissimilar Materials under Various Mechanical Loadings

Khairum Bin Hamzah [1] , **Nik Mohd Asri Nik Long** [2,3,*] , **Norazak Senu** [2,3] and **Zainidin K. Eshkuvatov** [4]

1 Fakulti Teknologi Kejuruteraan Mekanikal dan Pembuatan, Universiti Teknikal Malaysia Melaka, Hang Tuah Jaya, Durian Tunggal, Melaka 76100, Malaysia; khairum@utem.edu.my
2 Mathematics Department, Faculty of Science, Universiti Putra Malaysia, Serdang, Selangor 43400, Malaysia; norazak@upm.edu.my
3 Laboratory of Computational Sciences and Mathematical Physics, Institute for Mathematical Research, Universiti Putra Malaysia, Serdang, Selangor 43400, Malaysia
4 Faculty of Ocean Engineering Technology and Informatics, Universiti Malaysia Terengganu, Kuala Terengganu 21030, Malaysia; zainidin@umt.edu.my
* Correspondence: nmasri@upm.edu.my

Abstract: A new mathematical model is developed for the analytical study of two cracks in the upper plane of dissimilar materials under various mechanical loadings, i.e., shear, normal, tearing and mixed stresses with different geometry conditions. This problem is developed into a new mathematical model of hypersingular integral equations (HSIEs) by using the modified complex potentials (MCPs) function and the continuity conditions of the resultant force and displacement with the crack opening displacement (COD) function as the unknown. The newly obtained mathematical model of HSIEs are solved numerically by utilizing the appropriate quadrature formulas. Numerical computations and graphical demonstrations are carried out to observe the profound effect of the elastic constants ratio, mode of stresses and geometry conditions on the dimensionless stress intensity factors (SIFs) at the crack tips.

Keywords: two cracks; dissimilar materials; hypersingular integral equations; stress intensity factors

1. Introduction

Study on the vigor of materials and engineering structures provides a broad sense which is related to a review of the carrying capacity of a body with and without consideration of initial cracks. In order to predict the stress state or stress intensity in the vicinity of the crack tip due to the mechanical loading or residual stresses, one needs to determine very important factors, i.e., stress intensity factors (SIFs). The SIF is a fundamental parameter in fracture mechanics, and it is an important factor for safety analysis of the materials, structural stability and design analysis. Complex potential function (CPF) method introduced by Muskhelishvili [1] is the simplest and most rigorous method to investigate the behavior of SIFs, measured at the tip of cracks to determine the stability behavior of bodies or materials containing cracks or flaws. Many researchers used CPF methods to investigate the crack problems in an infinite plane [2–4], finite plane [5,6] and half plane [7–9]. Gray et al. [2] and Nik Long et al. [3] established the relevant hypersingular integral equations (HSIEs) using CPF method in calculating the SIFs with Green's function, and crack opening displacement (COD) function as the unknown, respectively. Liu et al. [4] analyzed SIFs for two unequal-length collinear cracks using weight functions method with COD function as the unknown. Lai and Schijve [5] analyzed a single hole-edge crack in a finite plane using CPF methods with the treatment of boundary condition with the minimum potential energy principle. Moreover, Zhang et al. [6] analyzed multiple cracks in a finite plane by numerically solved a system of singular integral equations with the Gauss–Chebyshev quadrature, and evaluating the SIFs. Legros et al. [7] performed the analysis of multiple circular inclusions in an elastic half plane based on complex singular integral equation with

the unknown tractions at each circular boundary approximated by a truncated complex Fourier series. Liu and Guo [8] used the CPF method to calculate the SIFs for the interaction between a screw dislocation and an oblique edge crack in a half plane with the help of Cauchy integral formula. Elfakhakhre et al. [9] investigated the behavior of the SIFs at the crack tips in half plane elasticity using the modified complex potentials (MCPs) with the distribution dislocation as the unknown function. As per the authors' knowledge, no mathematical model of the HSIEs has been made to date to develop and study the crack phenomenon in dissimilar materials under various mechanical loadings using CPF method.

Many different methods were applied by the researchers to investigate the crack problems in dissimilar materials. Chen [10] used the Fredholm integral equations to evaluate the dimensionless SIFs for multiple inclined cracks in dissimilar materials under shear stress. It was obtained that the mathematical model for the multiple cracks in dissimilar materials were reduced to the model in an infinite plane when $G_1 = G_2$. According to Chen and Hasebe [11], the values of dimensionless SIFs depend on the elastic constant ratio and crack geometric. They used the mixed boundary value problems to obtain a logarithmic singular kernel for a circular arc crack in the upper plane of dissimilar materials. Isida and Noguchi [12] analyzed the crack problems in dissimilar materials by using the continuous distributions of the body force method along the cracks but excluded the interface cracks and singularity problems for cracks terminating at the interface. Zhou et al. [13] found that the dimensionless SIFs for an arbitrary crack problems in dissimilar materials depends on the thickness of the strip, crack configuration and the existence of the crack near the punch foundation. They used a system of complex Cauchy type singular integral equations. Long and Xu [14] applied the combination of direct boundary integral method and displacement discontinuity method to solve the crack problems in dissimilar materials. The result showed that the proposed method was efficient especially for the scaled thin layers in the application of practical hydraulic fracturing simulations. Hamzah et al. [15,16] used the HSIEs to calculate the dimensionless SIFs for multiple cracks in the upper plane and both upper and lower planes of dissimilar materials subjected to shear stress. They expanded their study to analyze the behavior of dimensionless SIFs under various mechanical loadings, however it focused on a single crack in the upper plane of dissimilar materials [17].

The present mathematical model is a novel investigation of dimensionless SIFs at the crack tip of the two cracks in the upper plane of dissimilar materials under various mechanical loadings such as shear, normal, tearing and mixed stresses with different geometry conditions. By using CPF method, the problem is formulated into HSIEs. The noticeable impact of elastic constants ratio, mechanical loading and geometry conditions on SIFs for dissimilar materials has been depicted by means of numerical computations and graphical demonstrations. Moreover, a comparative analysis is carried out for dimensionless SIFs in dissimilar materials under various mechanical loadings to elucidate the unrevealed facts. The present findings may assist engineers in investigating the stability behavior of the perfectly bonded dissimilar structures or materials under various mechanical loadings.

2. Mathematical Model of the Problem

The CPF method plays an important role in solving the crack problems in plane elasticity [1]. In this method, the stress components $(\sigma_x, \sigma_y, \sigma_{xy})$, resultant force function $f(X, Y)$ and displacements (u, v) are related to two complex potentials $\Phi(z) = \phi'(z)$ and $\Omega(z) = \omega'(z)$ as follows

$$\sigma_y - i\sigma_{xy} = \Phi(z) + (z - \bar{z})\overline{\Phi'(z)} + \Omega(\bar{z}), \tag{1}$$

$$f = -Y + iX = \phi(z) + (z - \bar{z})\overline{\Phi'(z)} + \omega(\bar{z}), \tag{2}$$

$$2G(u + iv) = \kappa\phi(z) - (z - \bar{z})\overline{\Phi(z)} - \omega(\bar{z}), \tag{3}$$

$$\omega(z) = z\overline{\Phi}(z) + \overline{\psi}(z), \tag{4}$$

where $z = x + iy$, G is shear modulus of elasticity, $\kappa = (3 - v)/(1 + v)$ for plane stress, $\kappa = 3 - 4v$ for plane strain and v is Poisson's ratio. The derivative of Equation (2) with respect to z gives

$$\frac{d}{dz}\{-Y + iX\} = \Phi(z) + (z - \bar{z})\overline{\Phi''(z)}\frac{d\bar{z}}{dz} + \Omega(\bar{z})\frac{d\bar{z}}{dz} = N + iT \tag{5}$$

where the traction $N + iT$ denotes the normal and tangential components along the crack segment $\overline{z, z + dz}$. Note that the traction $N + iT$ depends on the position of point z and the direction of the segment $d\bar{z}/dz$.

According to Nik Long and Eshkuvatov [3], the complex potentials for a crack L in an infinite plane can be expressed by

$$\phi(z) = \frac{1}{2\pi} \int_L \frac{g(t)dt}{t - z}, \tag{6}$$

$$\omega(z) = \frac{1}{2\pi} \int_L \frac{z\overline{g(t)}d\bar{t}}{(\bar{t} - z)^2} + \frac{1}{2\pi} \int_L \frac{\overline{g(t)}dt}{\bar{t} - z} + \frac{1}{2\pi} \int_L \frac{g(t)d\bar{t}}{\bar{t} - z} - \frac{1}{2\pi} \int_L \frac{t\overline{g(t)}d\bar{t}}{(\bar{t} - z)^2}, \tag{7}$$

where $g(t)$ is COD function defined by

$$g(t) = \frac{2G}{i(\kappa + 1)}\left[(u(t) + iv(t))^+ - (u(t) + iv(t))^-\right], \tag{8}$$

$(u(t) + iv(t))^+$ and $(u(t) + iv(t))^-$ denote the displacements at point t of the upper and lower crack faces, respectively. Note that COD function has the following properties

$$g(t) = O\left[\sqrt{t - t_{A_j}}\right], \tag{9}$$

at the crack tip A_j, where $j = 1, 2$.

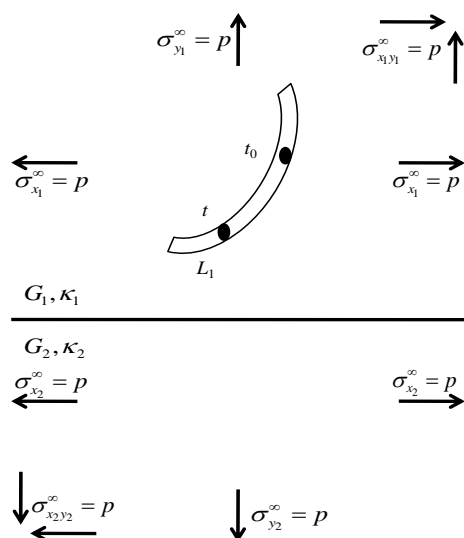Consider a crack in upper plane of dissimilar materials under various mechanical loadings; see Figure 1.

Figure 1. A crack L_1 in dissimilar materials under various mechanical loadings.

The conditions for strain components ε in dissimilar materials are

$$\varepsilon_{x_1} = \varepsilon_{x_2}, \quad \varepsilon_{y_1} = \varepsilon_{y_2}, \quad \varepsilon_{x_1 y_1} = \varepsilon_{x_2 y_2} \quad \text{and} \quad \varepsilon_{x_1} = \varepsilon_{x_2} = \varepsilon_{y_1} = \varepsilon_{y_2} \tag{10}$$

where subscripts 1 and 2 are the strain components for the upper and lower planes of dissimilar materials, respectively. Those strains can be defined by Young's modulus of elasticity E and stress components σ as

$$\varepsilon_{x_1} = \frac{1}{E_1}\left(\sigma_{x_1}^\infty - v_1\sigma_{y_1}^\infty\right), \qquad \varepsilon_{x_2} = \frac{1}{E_2}\left(\sigma_{x_2}^\infty - v_2\sigma_{y_2}^\infty\right), \tag{11}$$

$$\varepsilon_{y_1} = \frac{1}{E_1}\left(\sigma_{y_1}^\infty - v_1\sigma_{x_1}^\infty\right), \qquad \varepsilon_{y_2} = \frac{1}{E_2}\left(\sigma_{y_2}^\infty - v_2\sigma_{x_2}^\infty\right), \tag{12}$$

$$\varepsilon_{x_1y_1} = \frac{1+v_1}{E_1}\sigma_{x_1y_1}^\infty, \qquad \varepsilon_{x_2y_2} = \frac{1+v_2}{E_2}\sigma_{x_2y_2}^\infty, \tag{13}$$

and

$$\begin{aligned} \varepsilon_{x_1} = \varepsilon_{y_1} &= \frac{1-v_1}{E_1}\sigma_{x_1}^\infty = \frac{1-v_1}{E_1}\sigma_{y_1}^\infty, \\ \varepsilon_{x_2} = \varepsilon_{y_2} &= \frac{1-v_2}{E_2}\sigma_{x_2}^\infty = \frac{1-v_2}{E_2}\sigma_{y_2}^\infty, \end{aligned} \tag{14}$$

where $E_i = 2G_i(1+v_i)$ and $i = 1, 2$. For the shear stress, we have $\sigma_{x_1} = \sigma_{x_2} = p$, $\sigma_{y_1}^\infty = 0$, $\sigma_{y_2}^\infty = 0$ and applying condition Equation (10), Equation (11) is reduced to

$$\frac{1}{E_1}\sigma_{x_1}^\infty = \frac{1}{E_2}\sigma_{x_2}^\infty. \tag{15}$$

For normal stress, we have $\sigma_{y_1} = \sigma_{y_2} = p$, $\sigma_{x_1}^\infty = 0$, $\sigma_{x_2}^\infty = 0$ and applying condition Equation (10), Equation (12) is reduced to

$$\frac{1}{E_1}\sigma_{y_1}^\infty = \frac{1}{E_2}\sigma_{y_2}^\infty. \tag{16}$$

For tearing stress, we have $\sigma_{x_1y_1} = \sigma_{x_2y_2} = p$ and applying condition Equation (10), Equation (13) is reduced to

$$\frac{1+v_1}{E_1}\sigma_{x_1y_1}^\infty = \frac{1+v_2}{E_2}\sigma_{x_2y_2}^\infty. \tag{17}$$

Whereas for mixed stress, we have $\sigma_{x_1} = \sigma_{x_2} = \sigma_{y_1} = \sigma_{y_2} = p$ and applying condition Equation (10), Equation (14) is reduced to

$$\frac{1-v_1}{E_1}\sigma_{x_1}^\infty = \frac{1-v_2}{E_2}\sigma_{x_2}^\infty \quad \text{or} \quad \frac{1-v_1}{E_1}\sigma_{y_1}^\infty = \frac{1-v_2}{E_2}\sigma_{y_2}^\infty. \tag{18}$$

According to Chen and Hasebe [11], the MCPs for the crack in the upper plane of dissimilar materials are defined as

$$\phi_1(z) = \phi_{1p}(z) + \phi_{1c}(z), \qquad \psi_1(z) = \psi_{1p}(z) + \psi_{1c}(z) \tag{19}$$

where $\phi_{1p}(z)$ and $\psi_{1p}(z)$ are the principal parts and $\phi_{1c}(z)$ and $\psi_{1c}(z)$ are the complementary parts of the complex potentials. The complex potentials for the lower plane are represented by $\phi_2(z)$ and $\psi_2(z)$. Note that $\phi_{1p}(z)$ and $\psi_{1p}(z)$ are similar to the complex potentials for cracks in an infinite material. The continuity conditions for the resultant force (2) and displacement functions (3), yields

$$\{-Y + iX\}^+ = \{-Y + iX\}^-,$$

$$\left\{\phi_1(t) + (t-\bar{t})\overline{\Phi_1'(t)} + \omega_1(\bar{t})\right\}^+ = \left\{\phi_2(t) + (t-\bar{t})\overline{\Phi_2'(t)} + \omega_2(\bar{t})\right\}^-, \tag{20}$$

and

$$\{u + iv\}^+ = \{u + iv\}^-,$$

$$G_2\left\{\kappa_1\phi_1(t) - (t - \bar{t})\overline{\Phi_1(t)} - \omega_1(\bar{t})\right\}^+ = G_1\left\{\kappa_2\phi_2(t) - (t - \bar{t})\overline{\Phi_2(t)} - \omega_2(\bar{t})\right\}^-, \qquad (21)$$

where $t \in L_j$, $(j = 1, 2)$ and $+$ and $-$ signs represent the upper and lower planes of dissimilar materials, respectively. Apply Equations (19) and (4) into Equations (20) and (21), the following expressions are obtainable

$$\phi_{1c}(z) = \beta_1\left(z\overline{\phi'_{1p}}(z) + \overline{\psi_{1p}}(z)\right), \qquad z \in S_1 + L_b \qquad (22)$$

$$\psi_{1c}(z) = \beta_2\overline{\phi_{1p}}(z) - \beta_1\left(z\overline{\phi'_{1p}}(z) + z^2\overline{\phi''_{1p}}(z) + z\overline{\psi'_{1p}}(z)\right), \qquad z \in S_1 + L_b \qquad (23)$$

$$\phi_2(z) = \left(1 + \beta_2\right)\phi_{1p}(z), \qquad z \in S_2 + L_b \qquad (24)$$

$$\psi_2(z) = \left(\beta_1 - \beta_2\right)z\phi'_{1p}(z) + \left(1 + \beta_1\right)\psi_{1p}, \qquad z \in S_2 + L_b \qquad (25)$$

where $\overline{\phi_{1p}}(z) = \overline{\phi_{1p}(\bar{z})}$. Note that L_b is boundary of dissimilar materials, S_1 and S_2 are upper and lower planes of dissimilar materials, respectively, and β_1, β_2 are elastic constants defined as

$$\beta_1 = \frac{G_2 - G_1}{G_1 + \kappa_1 G_2}, \qquad \beta_2 = \frac{\kappa_1 G_2 - \kappa_2 G_1}{G_2 + \kappa_2 G_1}.$$

Consider two cracks L_1 and L_2 in the upper plane of dissimilar materials under various mechanical loadings; see Figure 2.
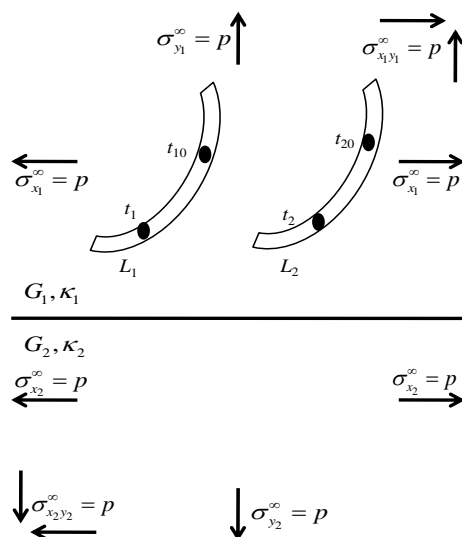

Figure 2. Two cracks L_1 and L_2 in the upper plane of dissimilar materials.

In order to develop the new mathematical model of HSIEs for two cracks in the upper plane of dissimilar materials, we need to define four traction components $\{N(t_{10}) + iT(t_{10})\}_{11}$, $\{N(t_{10}) + iT(t_{10})\}_{12}$, $\{N(t_{20}) + iT(t_{20})\}_{22}$ and $\{N(t_{20}) + iT(t_{20})\}_{21}$ which consist of two groups of $N + iT$ by using Equation (5). The first two tractions $\{N(t_{10}) + iT(t_{10})\}_{11}$ and $\{N(t_{20}) + iT(t_{20})\}_{21}$ are obtained when the observation point is placed at the point $t_{10} \in L_1$ and $t_{20} \in L_2$, respectively, caused by $g_1(t_1)$ at $t_1 \in L_1$. Whereas, the second two tractions $\{N(t_{10}) + iT(t_{10})\}_{12}$ and $\{N(t_{20}) + iT(t_{20})\}_{22}$ are obtained when the observation point is placed at the point $t_{10} \in L_1$ and $t_{20} \in L_2$, respectively, caused by $g_2(t_2)$ at $t_2 \in L_2$. Since both cracks lie in the upper part

of dissimilar materials, we need to combine four traction components which consist of the principal $\{N(t_{j0}) + iT(t_{j0})\}_{jp}$ $(j = 1, 2)$ and complementary parts $\{N(t_{j0}) + iT(t_{j0})\}_{jc}$ $(j = 1, 2)$. By using the superposition principle, the new mathematical model of HSIEs for two cracks in the upper plane of dissimilar materials can be obtained as follows

$$
\begin{aligned}
\{N(t_{10}) + iT(t_{10})\}_1 &= \{N(t_{10}) + iT(t_{10})\}_{11} + \{N(t_{10}) + iT(t_{10})\}_{12} \\
&= \frac{1}{\pi} \oint_{L_1} \frac{g_1(t_1)dt_1}{(t_1 - t_{10})^2} + \frac{1}{2\pi} \int_{L_1} K_1(t_1, t_{10})g_1(t_1)dt_1 + \frac{1}{2\pi} \int_{L_1} K_2(t_1, t_{10})\overline{g_1(t_1)}dt_1 \\
&\quad + \frac{1}{\pi} \int_{L_2} \frac{g_2(t_2)dt_2}{(t_2 - t_{10})^2} + \frac{1}{2\pi} \int_{L_2} K_1(t_2, t_{10})g_2(t_2)dt_2 + \frac{1}{2\pi} \int_{L_2} K_2(t_2, t_{10})\overline{g_2(t_2)}dt_2,
\end{aligned} \tag{26}
$$

$$
\begin{aligned}
\{N(t_{20}) + iT(t_{20})\}_2 &= \{N(t_{20}) + iT(t_{20})\}_{22} + \{N(t_{20}) + iT(t_{20})\}_{21} \\
&= \frac{1}{\pi} \oint_{L_2} \frac{g_2(t_2)dt_2}{(t_2 - t_{20})^2} + \frac{1}{2\pi} \int_{L_2} K_1(t_2, t_{20})g_2(t_2)dt_2 + \frac{1}{2\pi} \int_{L_2} K_2(t_2, t_{20})\overline{g_2(t_2)}dt_2 \\
&\quad + \frac{1}{\pi} \int_{L_1} \frac{g_1(t_1)dt_1}{(t_1 - t_{20})^2} + \frac{1}{2\pi} \int_{L_1} K_1(t_1, t_{20})g_1(t_1)dt_1 + \frac{1}{2\pi} \int_{L_1} K_2(t_1, t_{20})\overline{g_1(t_1)}dt_1,
\end{aligned} \tag{27}
$$

where

$$
\begin{aligned}
K_1(t_i, t_{j0}) &= \frac{1}{(t_i - t_{j0})^2}\left(\frac{(t_i - t_{j0})^2}{(\bar{t}_i - \bar{t}_{j0})^2}\frac{d\bar{t}_i}{dt_i}\frac{d\bar{t}_{j0}}{dt_{j0}} - 1\right) + \beta_1\left(\frac{1}{(t_i - \bar{t}_{j0})^2} + \frac{2(\bar{t}_{j0} - \bar{t}_i)}{(t_i - \bar{t}_{j0})^3}\right. \\
&\quad + \frac{d\bar{t}_{j0}}{dt_{j0}}\left(\frac{2(2t_{j0} - 3\bar{t}_{j0} + \bar{t}_i)}{(t_i - \bar{t}_{j0})^3} - \frac{6(\bar{t}_{j0} - \bar{t}_i)(\bar{t}_{j0} - t_{j0})}{(t_i - \bar{t}_{j0})^4} - \frac{1}{(t_i - \bar{t}_{j0})^2}\right)\right) + \beta_2\frac{d\bar{t}_{j0}}{dt_{j0}}\frac{1}{(t_i - \bar{t}_{j0})^2} \\
&\quad + \beta_1\left(\frac{1}{(\bar{t}_i - t_{j0})^2} + \frac{1}{(t_i - \bar{t}_{j0})^2} - \frac{d\bar{t}_{j0}}{dt_{j0}}\left(\frac{1}{(t_i - \bar{t}_{j0})^2} + \frac{2(\bar{t}_{j0} - t_{j0})}{(t_i - \bar{t}_{j0})^3}\right)\right)\frac{d\bar{t}_i}{dt_i}, \\
K_2(t_i, t_{j0}) &= \frac{t_i - t_{j0}}{(\bar{t}_i - \bar{t}_{j0})^3}\left(\frac{(\bar{t}_i - \bar{t}_{j0})}{(t_i - t_{j0})}\left(\frac{d\bar{t}_i}{dt_i} + \frac{d\bar{t}_{j0}}{dt_{j0}}\right) - 2\frac{d\bar{t}_i}{dt_i}\frac{d\bar{t}_{j0}}{dt_{j0}}\right) + \beta_1\left(\frac{1}{(\bar{t}_i - t_{j0})^2} + \frac{1}{(t_i - \bar{t}_{j0})^2}\right. \\
&\quad - \frac{d\bar{t}_{j0}}{dt_{j0}}\left(\frac{1}{(t_i - \bar{t}_{j0})^2} + \frac{2(\bar{t}_{j0} - t_{j0})}{(t_i - \bar{t}_{j0})^3}\right)\right) + \beta_1\left(\frac{1}{(\bar{t}_i - t_{j0})^2} + \frac{2(t_{j0} - t_i)}{(\bar{t}_i - t_{j0})^3}\right)\frac{d\bar{t}_i}{dt_i},
\end{aligned}
$$

and $i, j = 1, 2$. In Equation (26), the first three integrals on the right hand side represent the traction influence on crack L_1 caused by COD function $g_1(t_1)$ on crack L_1. The next three integrals represent the traction influence on crack L_1 caused by COD function $g_2(t_2)$ on crack L_2. Whereas in Equation (27), the first three integrals on the right hand side represent the traction influence on crack L_2 caused by COD function $g_2(t_2)$ on crack L_2. The next three integrals represent the traction influence on crack L_2 caused by COD function $g_1(t_1)$ on crack L_1. Note that the first integral with the equal sign in Equations (26) and (27) represents the hypersingular integral and must be defined as a finite part integral. If $G_2 = 0$, then $\beta_1 = \beta_2 = -1$, Equations (26) and (27) reduce to the HSIEs for the two cracks in a half plane elasticity [18]. Whereas, if $G_1 = G_2$, then $\beta_1 = \beta_2 = 0$, Equations (26) and (27) reduce to the HSIEs for the two cracks in an infinite plane [3].

In order to solve the new mathematical model of HSIEs, the curved length coordinate method is used. Let

$$
H(s) = \frac{h(s)}{\sqrt{a^2 - s^2}}, \qquad h(s) = g(t)|_{t=t(s)}. \tag{28}
$$

Then the following quadrature formulas can be applied [19–22]

$$
\frac{1}{\pi} \oint_{-a}^{a} \frac{\sqrt{a^2 - s^2}H(s)ds}{(s - s_0)^2} \simeq \sum_{j=1}^{M+1} W_j(s_0)H(s_j), \tag{29}
$$

and

$$\frac{1}{\pi}\int_{-a}^{a}\sqrt{a^2-s^2}H(s)ds \simeq \frac{1}{M+2}\sum_{j=1}^{M+1}(a^2-s_0^2)H(s_j),\tag{30}$$

where $H(s)$ is a given function, $M \in \mathbb{Z}^+$,

$$s_j = a\cos\left(\frac{j\pi}{M+2}\right),\ j = 1, 2, ..., M+1,$$

and

$$W_j(s_0) = -\frac{2}{M+2}\sum_{n=0}^{M}(n+1)\sin\left(\frac{j\pi}{M+2}\right)\sin\left(\frac{(n+1)j\pi}{M+2}\right)U_n\left(\frac{s_{j0}}{a}\right),$$

and the observation points

$$s_0 = s_{0,k} = a\cos\left(\frac{k\pi}{M+2}\right),\ k = 1, 2, ..., M+1.$$

Here, $U_n(t)$ is a Chebyshev polynomial of the second kind, defined by

$$U_n(t) = \frac{\sin((n+1)\theta)}{\sin\theta},\text{where } t = \cos\theta.\tag{31}$$

The normal and tangential components $N + iT$ of the HSIEs for the shear stress $\sigma_{x_1} = \sigma_{x_2} = p$, normal stress $\sigma_{y_1} = \sigma_{y_2} = p$, tearing stress $\sigma_{x_1 y_1} = \sigma_{x_2 y_2} = p$ and mixed stress $\sigma_{x_1} = \sigma_{x_2} = \sigma_{y_1} = \sigma_{y_2} = p$ with an angle of the crack α are defined as follows

$$N + iT = -p\sin^2\alpha - ip\sin\alpha\cos\alpha,\tag{32}$$

$$N + iT = -p\cos^2\alpha + ip\sin\alpha\cos\alpha,\tag{33}$$

$$N + iT = 2p\sin\alpha\cos\alpha + ip(\cos^2\alpha - \sin^2\alpha),\tag{34}$$

$$N + iT = -p + i0.\tag{35}$$

In order to investigate the behavior of dimensionless SIFs for two cracks in the upper plane of dissimilar materials under various mechanical loadings, we define the SIFs at the crack tips A_j and B_j as follows

$$K_{A_j} = (K_1 - iK_2)_{A_j} = \sqrt{2\pi}\lim_{t\to t_{A_j}}\sqrt{|t - t_{A_j}|}g_1'(t_1),\qquad j = 1, 2,\tag{36}$$

$$K_{B_j} = (K_1 - iK_2)_{B_j} = \sqrt{2\pi}\lim_{t\to t_{B_j}}\sqrt{|t - t_{B_j}|}g_2'(t_2),\qquad j = 1, 2,\tag{37}$$

where $g_1'(t_1)$ and $g_2'(t_2)$ are defined as follows

$$g_k'(t_k)|_{t_k=t_k(s_k)} = \frac{-s_k H_k(s_k)}{\sqrt{a_k^2 - s_k^2}}e^{-i\theta_{A_j}},\qquad H_k'(s_k) = 0,\tag{38}$$

and $k = 1, 2$. Therefore, the dimensionless SIFs at crack tips A_j and B_j are defined as follows

$$K_{A_j} = (K_1 - iK_2)_{A_j} = \sqrt{2\pi}\lim_{s\to s_{A_j}}\sqrt{|s - s_{A_j}|}\left[\frac{-s_1 H_1(s_1)}{\sqrt{a_1^2 - s_1^2}}e^{-i\theta_{A_j}}\right] = \sqrt{a_1\pi}F_{A_j},\tag{39}$$

$$K_{B_j} = (K_1 - iK_2)_{B_j} = \sqrt{2\pi}\lim_{s\to s_{B_j}}\sqrt{|s - s_{B_j}|}\left[\frac{-s_2 H_2(s_2)}{\sqrt{a_2^2 - s_2^2}}e^{-i\theta_{B_j}}\right] = \sqrt{a_2\pi}F_{B_j},\tag{40}$$

where

$$F_{A_j} = H_1(-a_1)e^{-i\theta_{A_j}} = F_{1A_j} + iF_{2A_j},$$

$$F_{B_j} = H_2(-a_2)e^{-i\theta_{B_j}} = F_{1B_j} + iF_{2B_j}.$$

F_{1A_j} and F_{1B_j} are the Mode I dimensionless SIFs at crack tips A_j and B_j, respectively, and characterizes the amplitude of normal stress singularity. Whereas F_{2A_j} and F_{2B_j} are the Mode II dimensionless SIFs at crack tips A_j and B_j, respectively, and describe the amplitude of the shear stress singularity. Note that the crack propagates if the value of dimensionless SIFs is greater than or equal to the value of critical dimensionless SIFs [23]. The strength of the materials is getting weaker as the value of dimensionless SIFs increases [24]. Whereas the negative values of dimensionless SIFs were obtained for some geometric problems, implicatively insinuating the possible use of unknown contact and frictional stresses between the closed crack surfaces, thereby invalidating the presumption of a frictionless open crack model [25].

3. Numerical Results and Discussion

In this section, numerical computations and graphical demonstrations are carried out to show the effects of the elastic constants ratio, mode of stresses and geometry conditions on the dimensionless SIFs for crack problems in the upper plane of dissimilar materials. To validate the proposed mathematical model, we compared our numerical results with a crack parallel to the boundary of dissimilar materials investigated by Isida and Noguchi [12] in Table 1, and two cracks in the upper plane of dissimilar materials presented by Chen [10] in Table 2.

Consider the geometry conditions for crack problems in the upper plane of dissimilar materials under various mechanical loadings; see Figure 3.

Table 1 shows the dimensionless SIFs for a crack parallel to the boundary of dissimilar materials under normal stress when elastic constant ratio $G_2/G_1 = 4.0$ and $h/2R$ varies (Figure 3a). Our numerical results totally agree with those of Isida and Noguchi [12]. We observed that F_1 at crack tip A_1 is equal to F_1 at crack tip A_2. Whereas F_2 at crack tip A_1 is equal to the negative of F_2 at crack tip A_2. This is due to the equivalence of the stress acting at the tips of the cracks.
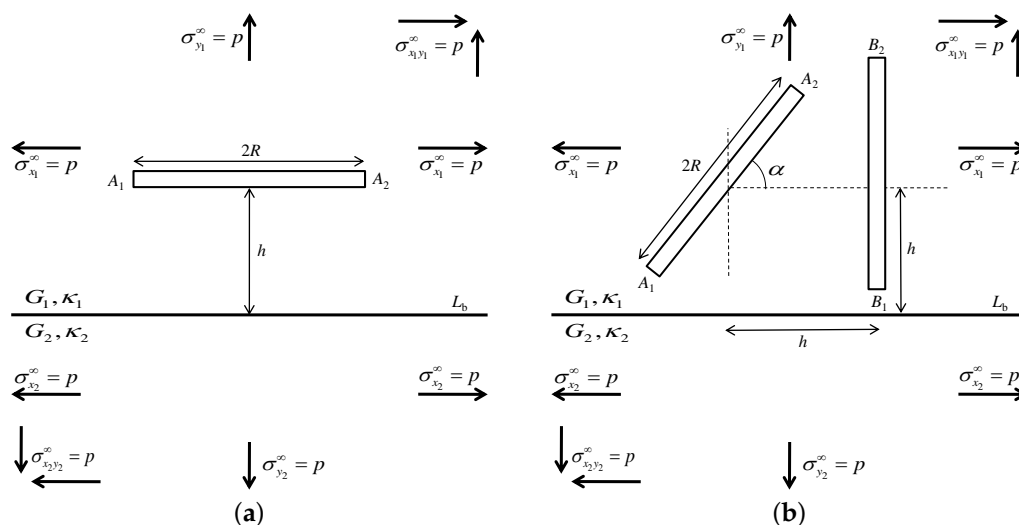

Figure 3. The geometry conditions for crack problems in the upper plane of dissimilar materials. (**a**) A crack parallel to the boundary; (**b**) Two cracks in the upper plane.

Table 1. Stress intensity factors (SIFs) for a crack parallel to the boundary of dissimilar materials (Figure 3a).

| SIF	h/2R						
	0.1	0.2	0.3	0.4	0.5	0.6	0.7
F_{1A_1} *	0.8083	0.8357	0.8568	0.8752	0.8920	0.9071	0.9203
F_{2A_1} *	0.1119	0.0811	0.0634	0.0500	0.0391	0.0304	0.0236
F_{1A_2} *	0.8083	0.8357	0.8568	0.8752	0.8920	0.9071	0.9203
F_{1A_2} **	0.8080	0.8360	0.8570	0.8750	0.8920	0.9070	0.9200
F_{2A_2} *	−0.1119	−0.0811	−0.0634	−0.0500	−0.0391	−0.0304	−0.0236
F_{2A_2} **	−0.1120	−0.0810	−0.0630	−0.0500	−0.0390	−0.0300	−0.0240

* Present study, ** Isida and Noguchi [12].

Table 2. SIFs for two cracks in the upper plane of dissimilar materials under various mechanical loadings (Figure 3b).

| Stress	G_2/G_1	SIF							
		F_{1A_1}	F_{2A_1}	F_{1A_2}	F_{2A_2}	F_{1B_1}	F_{2B_1}	F_{1B_2}	F_{2B_2}
Shear	0.2 *	0.4634	−0.3358	0.0612	−0.1974	1.2272	−0.0336	1.1004	0.0510
	0.2 **	0.4670	−0.3333	0.0420	−0.2010	1.2140	−0.0180	1.1010	0.0650
	1.0 *	0.4250	−0.3226	0.0420	−0.2341	0.8909	−0.0364	0.9844	0.0536
	1.0 **	0.4250	−0.3230	0.0420	−0.2360	0.8910	−0.0360	0.9850	0.0530
	5.0 *	0.4219	−0.3000	0.0571	−0.2352	0.6666	−0.0486	0.9128	0.0472
	5.0 **	0.4020	−0.2830	0.0370	−0.2400	0.6600	−0.0440	0.9030	0.0460
Normal	0.2 *	0.7333	0.5407	0.5561	0.6535	−0.1501	−0.1375	0.1483	−0.0758
	1.0 *	0.5177	0.4920	0.4833	0.5594	−0.1097	−0.0805	0.1152	−0.0270
	5.0 *	0.3974	0.4609	0.4327	0.5093	−0.0649	−0.0472	0.1122	−0.0079
Tearing	0.2 *	−1.3748	0.2490	−1.0732	0.0420	0.4691	−1.1090	−0.0698	−1.1981
	1.0 *	−1.1290	0.1528	−0.9643	0.0614	0.3696	−0.7944	−0.0589	−1.1132
	5.0 *	−0.9501	0.0443	−0.8446	0.0524	0.2347	−0.5754	−0.0770	−1.0218
Mixed	0.2 *	1.1967	0.2050	0.6173	0.4562	1.0771	−0.1711	1.2488	−0.0247
	1.0 *	0.9427	0.1694	0.5253	0.3254	0.7812	−0.1169	1.0996	0.0266
	5.0 *	0.8194	0.1609	0.4898	0.2741	0.6017	−0.0958	1.0250	0.0393

* Present study, ** Chen [10].

Table 2 shows the dimensionless SIFs for two cracks in the upper plane of dissimilar materials under various mechanical loadings when $\alpha = 45°$ and $R/h = 0.9$ (Figure 3b). For shear stress, our numerical results agree with those of Chen [10]. For other stresses, the value of dimensionless SIFs are displayed in Figures 4–7. The dimensionless SIFs with black lines at crack tips A_1 and B_1, and with blue lines at crack tips A_2 and B_2 under shear stress are delineated in Figure 4. It is found that as G_2/G_1 increases, F_1 decreases at all cracks tips. However F_2 increases when $\alpha > 40°$ at tip A_1 and decreases at tip A_2. As α increases, F_1 increases at crack tips A_1 and A_2. These numerical evidences show that the materials become weaker as α increases and more stable as G_2/G_1 increases.
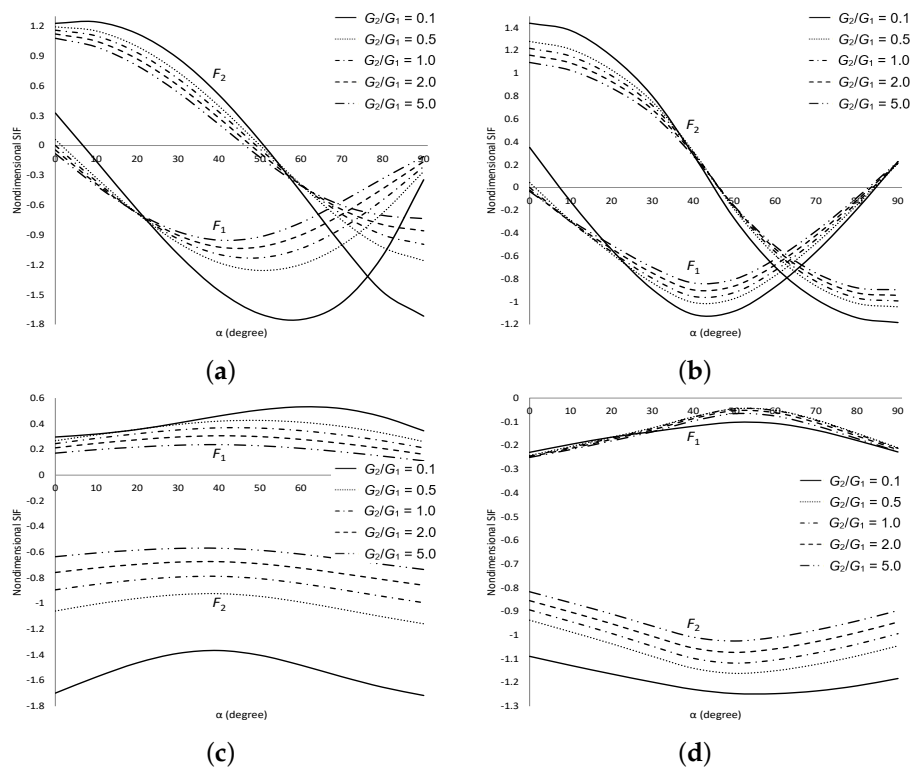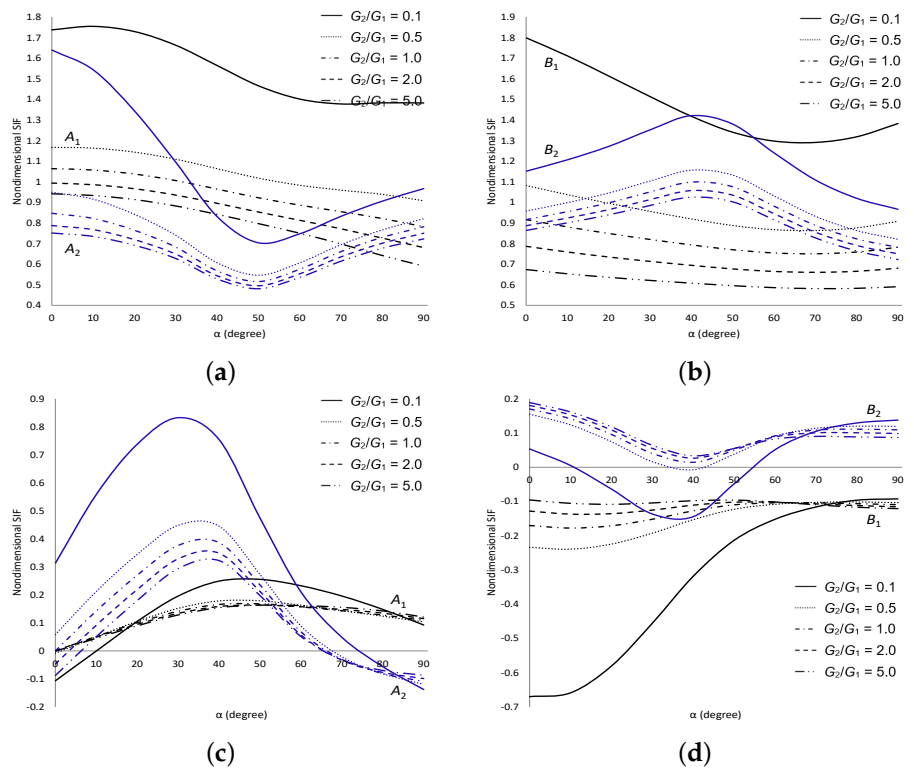

(a)

(b)
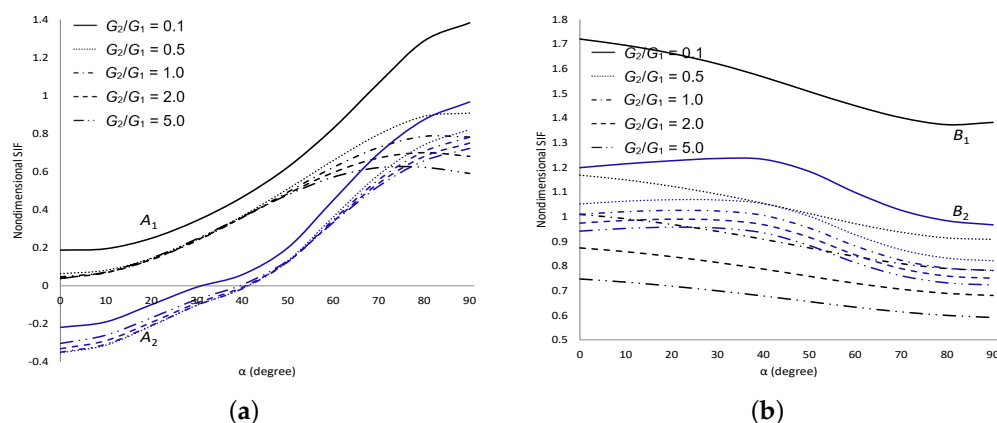
Figure 4. *Cont.*
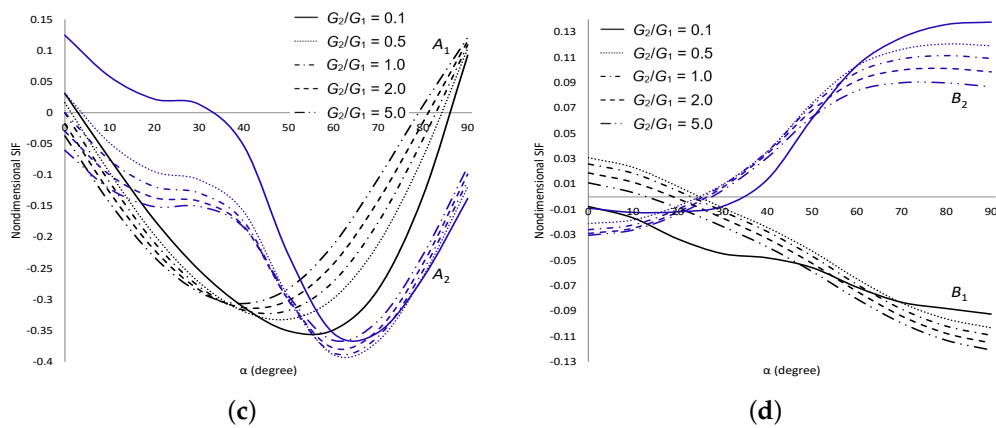
Figure 4. SIFs for two cracks in the upper plane of dissimilar materials under shear stress. (**a**) Dimensionless SIF F_1 at crack tips A_1 and A_2; (**b**) Dimensionless SIF F_1 at crack tips B_1 and B_2; (**c**) Dimensionless SIF F_2 at crack tips A_1 and A_2; (**d**) Dimensionless SIF F_2 at crack tips B_1 and B_2.
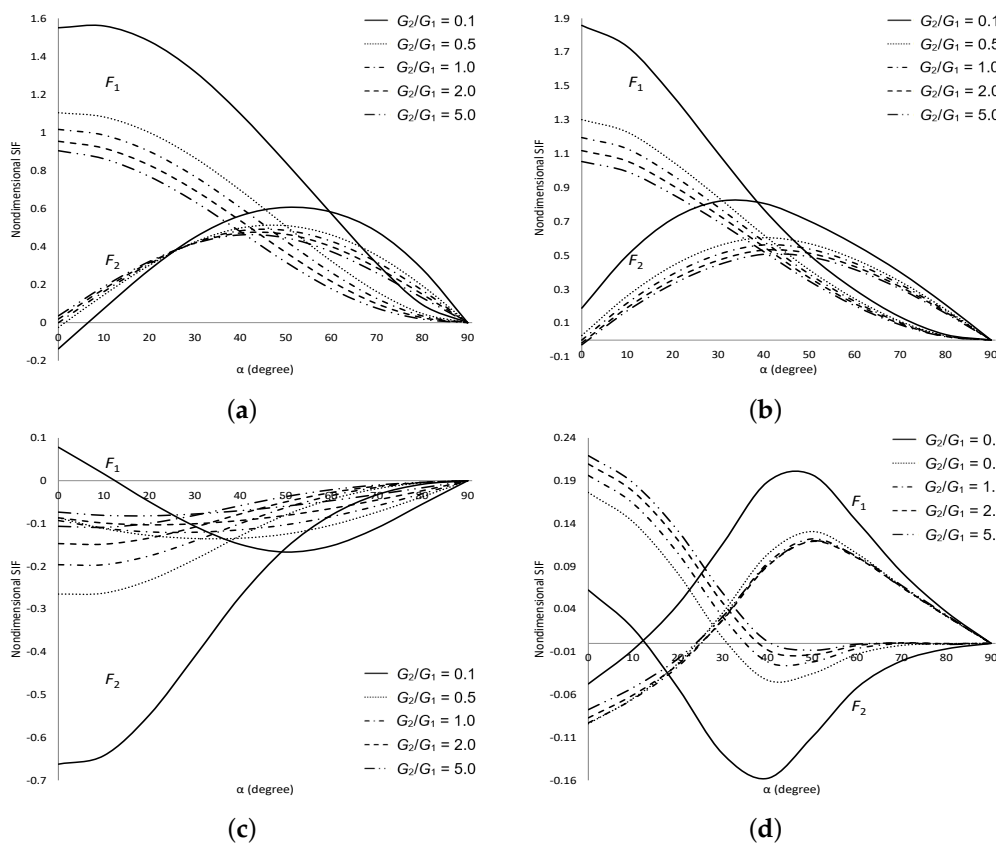
Figure 5. SIFs for two cracks in the upper plane of dissimilar materials under normal stress. (**a**) Crack tip A_1; (**b**) Crack tip A_2; (**c**) Crack tip B_1; (**d**) Crack tip B_2.

Figure 6. SIFs for two cracks in the upper plane of dissimilar materials under tearing stress. (**a**) Crack tip A_1; (**b**) Crack tip A_2; (**c**) Crack tip B_1; (**d**) Crack tip B_2.

Figure 7. SIFs for two cracks in the upper plane of dissimilar materials under mixed stress. (**a**) Dimensionless SIF F_1 at crack tips A_1 and A_2; (**b**) Dimensionless SIF F_1 at crack tips B_1 and B_2; (**c**) Dimensionless SIF F_2 at crack tips A_1 and A_2; (**d**) Dimensionless SIF F_2 at crack tips B_1 and B_2.

The dimensionless SIFs under normal stress are delineated in Figure 5. It is observed that as G_2/G_1 increases F_1 decreases at cracks tips A_1, A_2 and B_2, and increases at tip B_1. As α increases F_1 decreases at crack tips A_1 and A_2. Whereas as $\alpha = 90°$, the values of F_1 and F_2 are equal to zero at all cracks tips, due to the stress acting parallel to the geometric of the cracks. These observations show that the materials are more stable as α and G_2/G_1 increase. The dimensionless SIFs under tearing stress are delineated in Figure 6. It demonstrates that as G_2/G_1 increases, F_1 increases at cracks tips A_1, A_2 and B_1 but F_2 only increases at tips B_1 and B_2. As α increases, F_2 decreases at crack tips A_1 and A_2. These results indicate that the strength of the materials depends on α and G_2/G_1. The dimensionless SIFs with black lines at crack tips A_1 and B_1, and with blue lines at crack tips A_2 and B_2 under mixed stress are delineated in Figure 7. It portrays that as G_2/G_1 increases F_1 decreases at all cracks tips. As α increases, F_1 decreases at crack tips A_1 and B_1. These results enable us to conclude that the materials are more stable as G_2/G_1 increases.

Consider the geometry conditions for two cracks in the upper plane of dissimilar materials under various mechanical loadings as depicted in Figure 8.
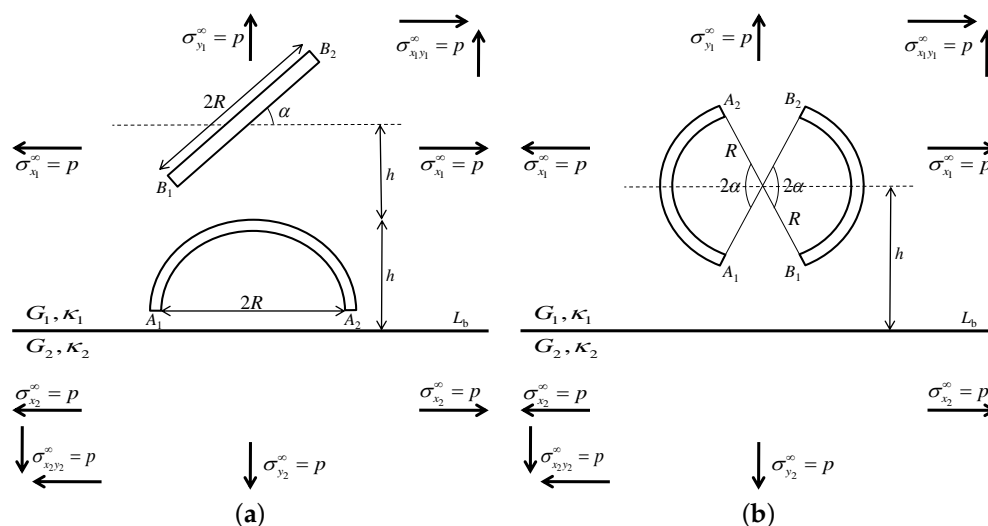

Figure 8. The geometry conditions for two cracks in the upper plane of dissimilar materials. (**a**) A semi circular arc crack and an inclined crack; (**b**) Two equal circular arc cracks on the same circle.

The dimensionless SIFs with black lines at crack tips A_1 and B_1, and with blue lines at crack tips A_2 and B_2 for a semi circular arc crack and an inclined crack in the upper plane of dissimilar materials under various mechanical loadings when $h = 1.5R$ and α varies are plotted in Figures 9–12 (Figure 8a).

The dimensionless SIFs under shear stress are delineated in Figure 9. It is found that as G_2/G_1 and α increase F_1 decreases and increases, respectively at all cracks tips. As G_2/G_1 increases, F_2 increases at crack tip A_1, decreases at tip A_2 and does not show any significant difference at tips B_1 and B_2. These numerical evidences show that the materials are more stable as G_2/G_1 increases and are getting weaker as α increases. The dimensionless SIFs under normal stress are delineated in Figure 10. It can be seen that as G_2/G_1 increases F_1 decreases at cracks tips B_1 and B_2 but at tips A_1 when $\alpha < 55°$ and A_2 when $\alpha < 80°$. As α increases, F_1 decreases at all cracks tips. These observations show that the materials are more stable as G_2/G_1 and α increase. The dimensionless SIFs under tearing stress are delineated in Figure 11. It portrays that as G_2/G_1 increases F_1 increases at all cracks tips. As α increases, F_1 decreases when $\alpha < 45°$ at all cracks tips. These results show that the strength of the materials depends on the values of G_2/G_1 and α. For mixed stress, the dimensionless SIFs are displayed in Figure 12. It is observed that as G_2/G_1 increases F_1 decreases at all cracks tips and F_2 decreases at crack tips A_2 and B_2. As α increases, F_1 does not show any significant difference at all cracks tips. These results enable us to conclude that the materials are more stable as G_2/G_1 increases.
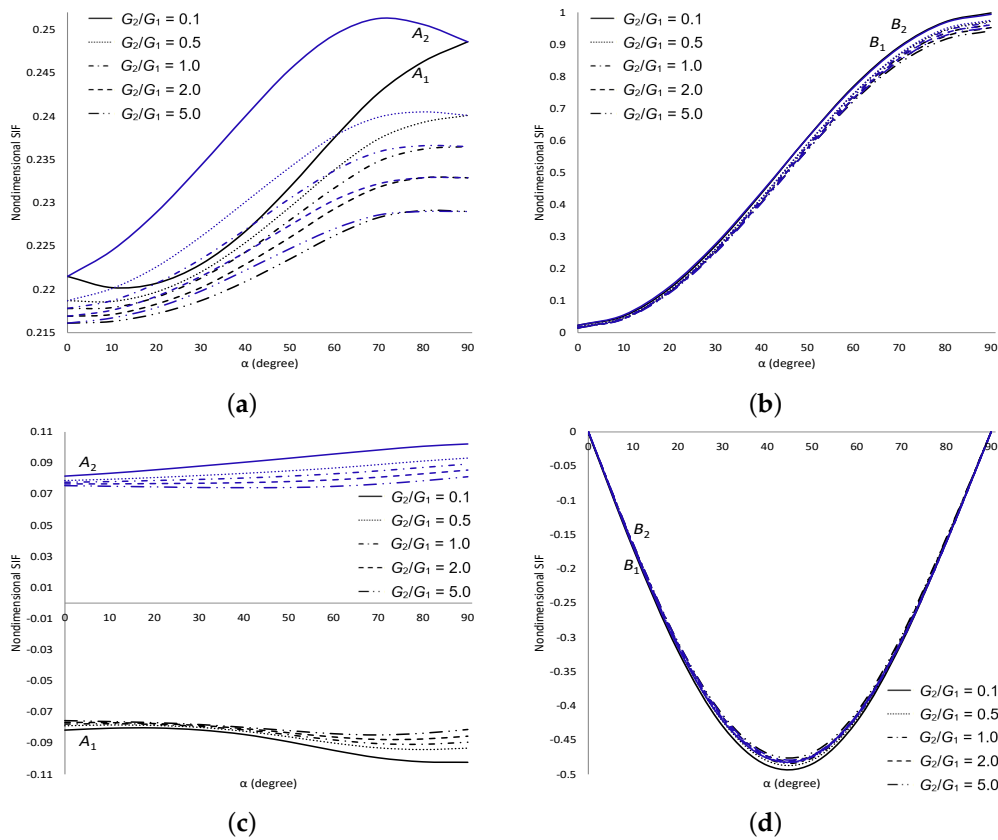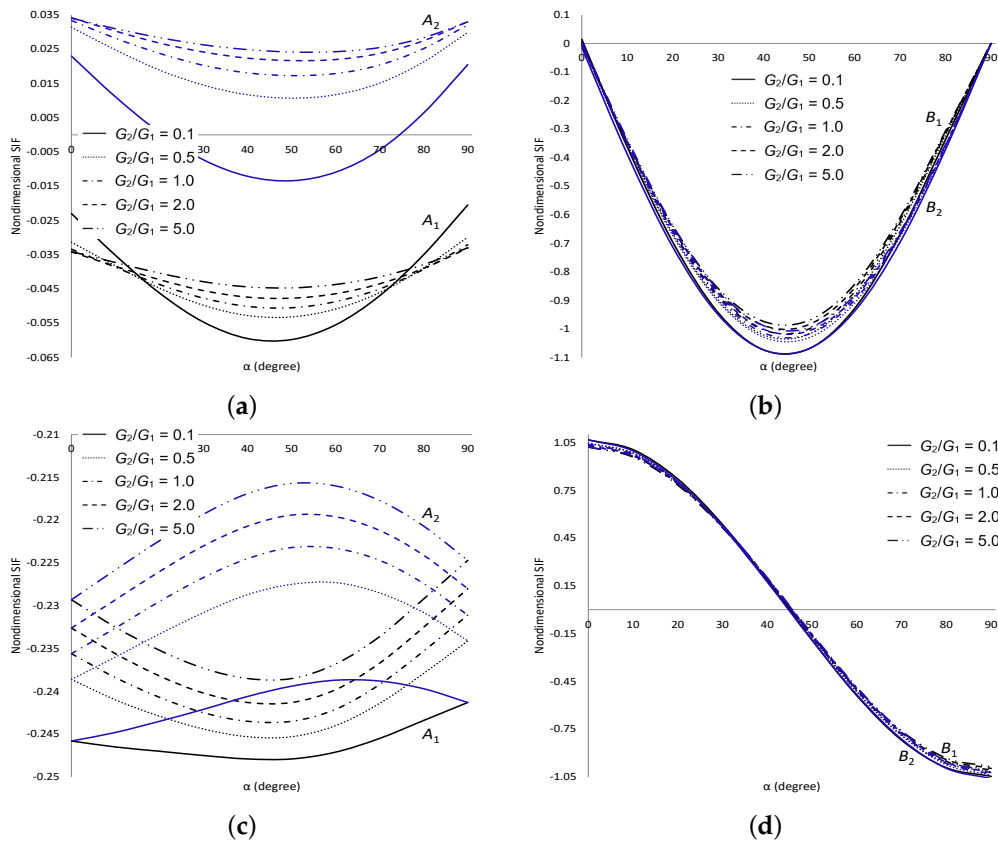
Figure 9. SIFs for two cracks in the upper plane of dissimilar materials under shear stress. (**a**) Dimensionless SIF F_1 at crack tips A_1 and A_2; (**b**) Dimensionless SIF F_1 at crack tips B_1 and B_2; (**c**) Dimensionless SIF F_2 at crack tips A_1 and A_2; (**d**) Dimensionless SIF F_2 at crack tips B_1 and B_2.

Figure 10. *Cont.*

(c)

(d)
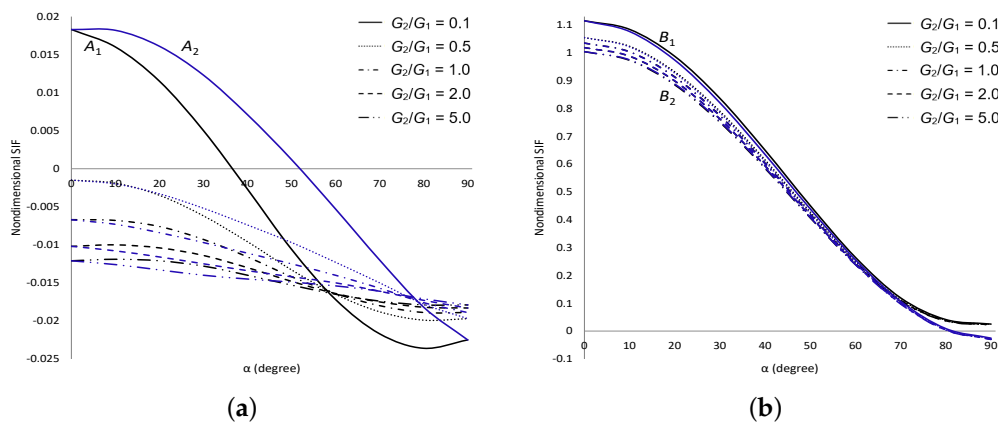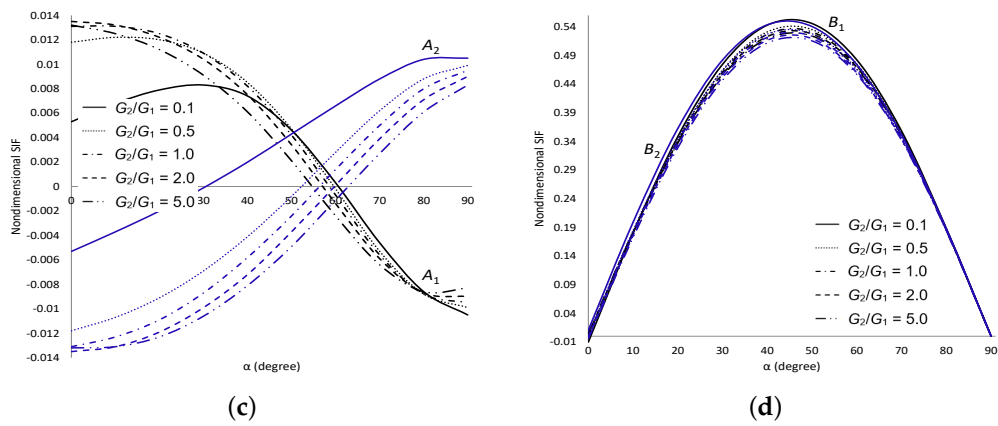
Figure 10. SIFs for two cracks in the upper plane of dissimilar materials under normal stress. (**a**) Dimensionless SIF F_1 at crack tips A_1 and A_2; (**b**) Dimensionless SIF F_1 at crack tips B_1 and B_2; (**c**) Dimensionless SIF F_2 at crack tips A_1 and A_2; (**d**) Dimensionless SIF F_2 at crack tips B_1 and B_2.
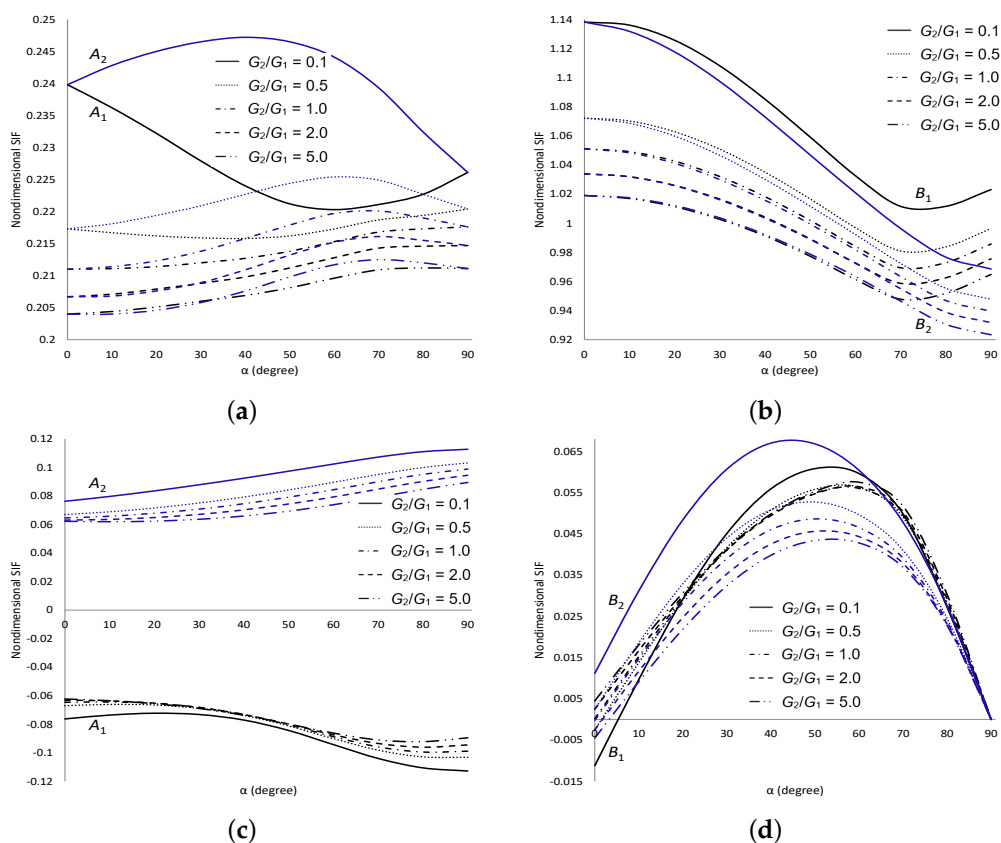

(a)

(b)

(c)

(d)

Figure 11. SIFs for two cracks in the upper plane of dissimilar materials under tearing stress. (**a**) Dimensionless SIF F_1 at crack tips A_1 and A_2; (**b**) Dimensionless SIF F_1 at crack tips B_1 and B_2; (**c**) Dimensionless SIF F_2 at crack tips A_1 and A_2; (**d**) Dimensionless SIF F_2 at crack tips B_1 and B_2.

Figure 12. SIFs for two cracks in the upper plane of dissimilar materials under mixed stress. (**a**) Dimensionless SIF F_1 at crack tips A_1 and A_2; (**b**) Dimensionless SIF F_1 at crack tips B_1 and B_2; (**c**) Dimensionless SIF F_2 at crack tips A_1 and A_2; (**d**) Dimensionless SIF F_2 at crack tips B_1 and B_2.

Figure 13 shows a comparison of the dimensionless SIFs for two equal circular arc cracks on the same circle in the upper plane of dissimilar materials under shear stress when $G_2/G_1 = 1.0$, $h = 1.5R$ and α varies (Figure 8b). Our numerical results agree with those of Chen and Hasebe [26]. We observed that the value of F_1 is equal at all crack tips. Whereas F_2 at crack tips A_1 and A_2 are equal to the negative of F_2 at crack tips B_1 and B_2, respectively. This is due to the equivalence of the stress acting at the tips of the cracks.
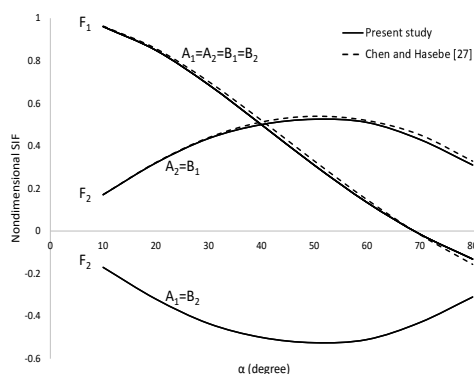

Figure 13. Comparison of dimensionless SIFs between present study and Chen and Hasebe [26] at all crack tips.

For other values of dimensionless SIFs under various mechanical loadings are presented in Figures 14–17. The dimensionless SIFs under shear stress are delineated in Figure 14. It is observed that F_1 at crack tips A_1 and A_2 are equal to F_1 at tips B_1 and B_2, respectively. Whereas F_2 at crack tips A_1 and A_2 are equal to the negative of F_2 at tips B_1

and B_2, respectively. As G_2/G_1 and α increase, F_1 decreases at all cracks tips. As G_2/G_1 increases, F_2 increases at crack tips A_1 and B_2, and decreases at tips A_2 and B_1. These observations show that the materials are more stable as G_2/G_1 and α increase.

The dimensionless SIFs under normal stress are delineated in Figure 15. It demonstrates that F_1 at crack tips A_1 and A_2 are equal to F_1 at tips B_1 and B_2, respectively. Whereas F_2 at crack tips A_1 and A_2 are equal to the negative of F_2 at tips B_1 and B_2, respectively. As G_2/G_1 and α increase, F_1 decreases and increases, respectively at all cracks tips. As α increases, F_2 increases at crack tips A_1 and B_2 when $\alpha < 45°$, and decreases at tips A_2 and B_1 when $\alpha < 45°$. These results show that the materials are more stable as G_2/G_1 increases and become weaker as α increases. The dimensionless SIFs under tearing stress are delineated in Figure 16. It is found that F_2 at crack tips A_1 and A_2 are equal to F_2 at tips B_1 and B_2, respectively. Whereas F_1 at crack tips A_1 and A_2 are equal to the negative of F_1 at tips B_1 and B_2, respectively. As G_2/G_1 increases, F_1 increases at crack tips A_1 and B_2, and decreases at tips A_2 and B_1. As α increases, F_1 decreases at crack tips A_1 and B_2 when $\alpha < 50°$, and increases at tips A_2 and B_1 when $\alpha < 50°$. Whereas F_2 increases at all cracks tips as α increases. These numerical evidences show that the materials are more stable as G_2/G_1 increases and become weaker as α increases. The dimensionless SIFs under mixed stress are delineated in Figure 17. It is obtained that F_1 at crack tips A_1 and A_2 are equal to F_1 at tips B_1 and B_2, respectively. Whereas F_2 at crack tips A_1 and A_2 are equal to the negative of F_2 at tips B_1 and B_2, respectively. As G_2/G_1 and α increase, F_1 decreases at all cracks tips. F_2 increases at crack tips A_1 and B_2, and decreases at tips A_2 and B_1 as G_2/G_1 increases. These numerical results show that the materials are more stable as G_2/G_1 and α increase.
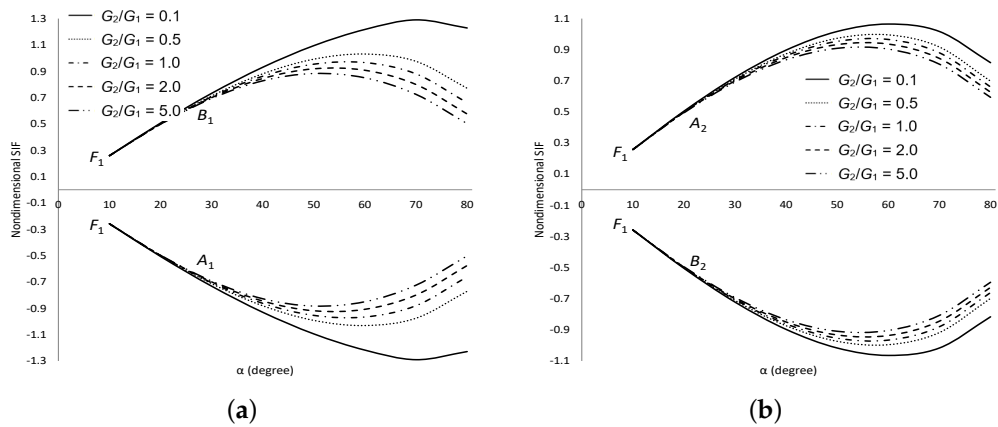

(**a**) Dimensionless SIF F_1 at crack tips A_1 and B_1 (**b**) Dimensionless SIF F_1 at crack tips A_2 and B_2

(**c**) Dimensionless SIF F_2 at crack tips A_1 and B_1 (**d**) Dimensionless SIF F_2 at crack tips A_2 and B_2
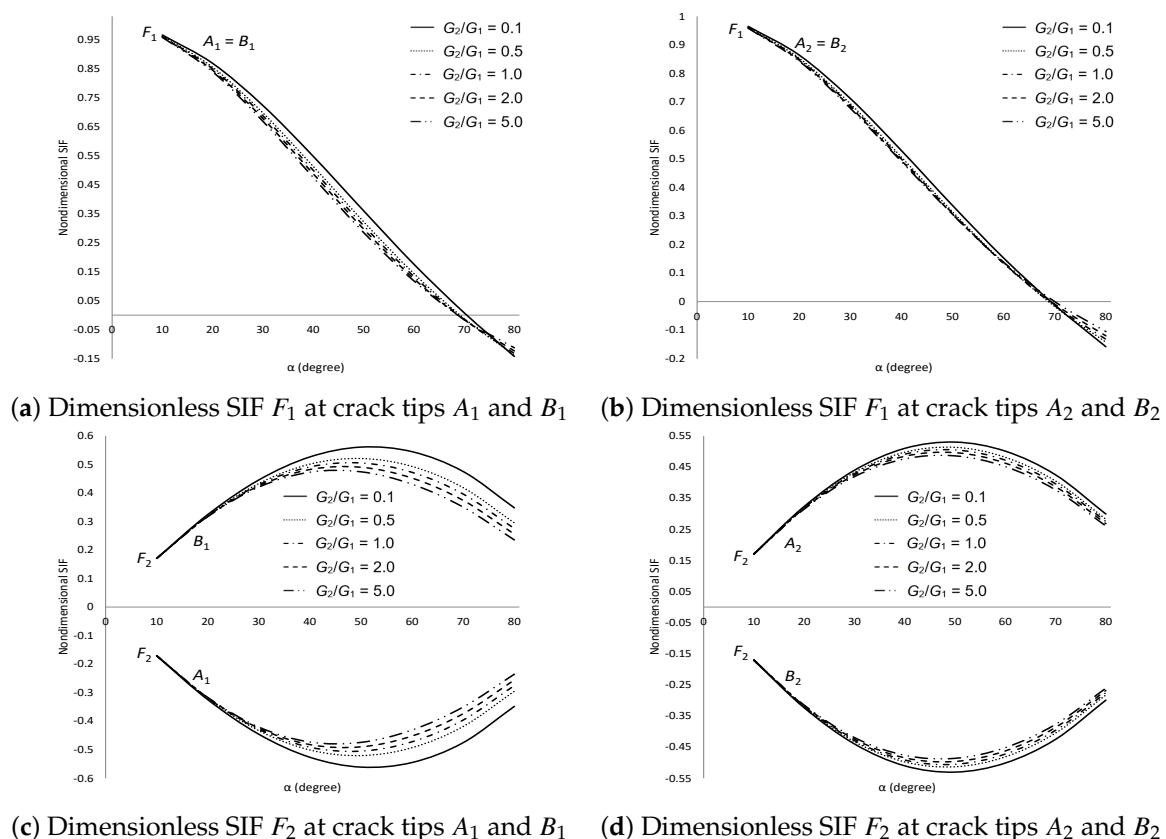
Figure 14. SIFs for two cracks in the upper plane of dissimilar materials under shear stress. (**a**) Dimensionless SIF F_1 at crack tips A_1 and B_1; (**b**) Dimensionless SIF F_1 at crack tips A_2 and B_2; (**c**) Dimensionless SIF F_2 at crack tips A_1 and B_1; (**d**) Dimensionless SIF F_2 at crack tips A_2 and B_2.
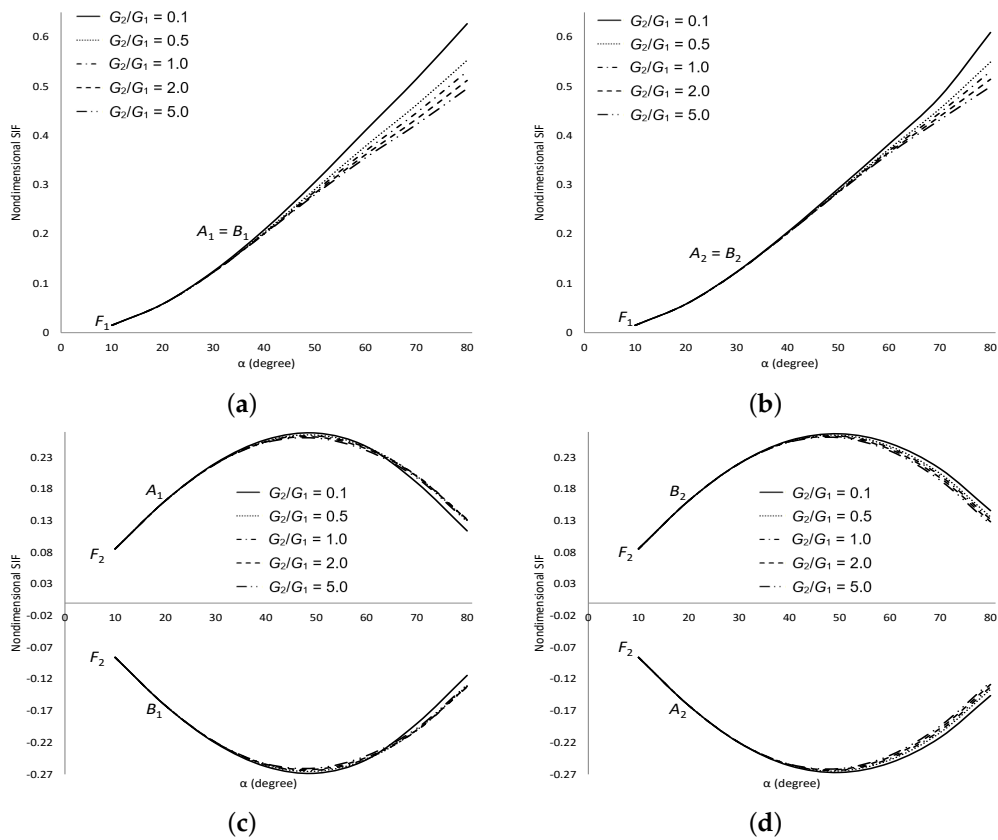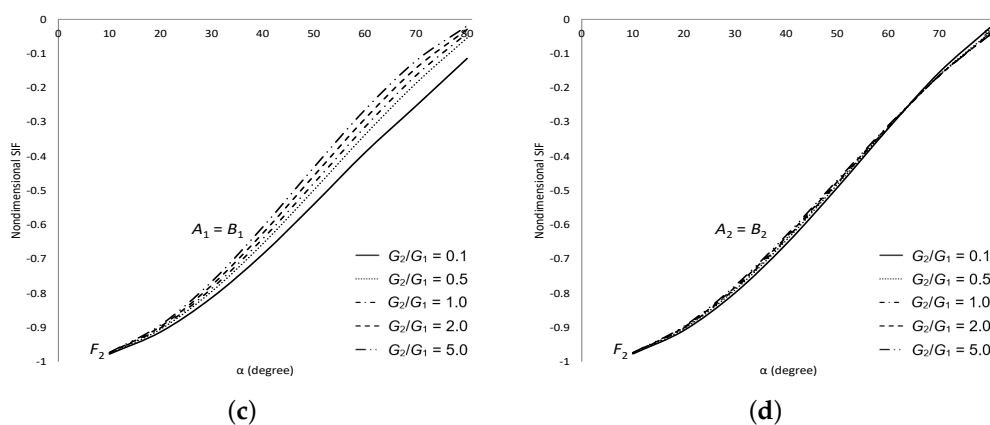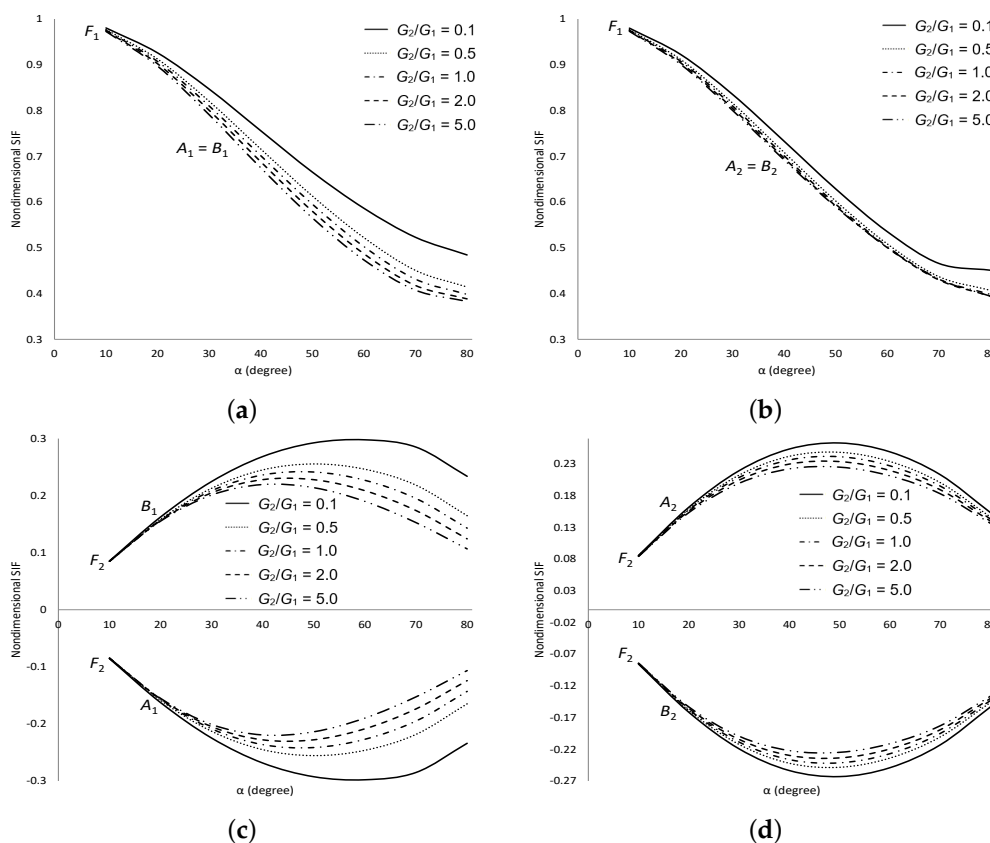
Figure 15. SIFs for two cracks in the upper plane of dissimilar materials under normal stress. (**a**) Dimensionless SIF F_1 at crack tips A_1 and B_1; (**b**) Dimensionless SIF F_1 at crack tips A_2 and B_2; (**c**) Dimensionless SIF F_2 at crack tips A_1 and B_1; (**d**) Dimensionless SIF F_2 at crack tips A_2 and B_2.

Figure 16. *Cont.*

(c)

(d)

Figure 16. SIFs for two cracks in the upper plane of dissimilar materials under tearing stress. (**a**) Dimensionless SIF F_1 at crack tips A_1 and B_1; (**b**) Dimensionless SIF F_1 at crack tips A_2 and B_2; (**c**) Dimensionless SIF F_2 at crack tips A_1 and B_1; (**d**) Dimensionless SIF F_2 at crack tips A_2 and B_2.

(a)

(b)

(c)

(d)

Figure 17. SIFs for cracks in the upper plane of dissimilar materials under mixed stress. (**a**) Dimensionless SIF F_1 at crack tips A_1 and B_1; (**b**) Dimensionless SIF F_1 at crack tips A_2 and B_2; (**c**) Dimensionless SIF F_2 at crack tips A_1 and B_1; (**d**) Dimensionless SIF F_2 at crack tips A_2 and B_2.

4. Conclusions

The present mathematical model is focused on the analytical investigation of dimensionless SIFs at the crack tip of two cracks problems in the upper plane of dissimilar materials under various mechanical loadings such as shear, normal, tearing and mixed stresses with different geometry conditions. The problem was formulated into a new mathematical model of HSIEs by using the MCPs function and the continuity conditions of the resultant force and displacement with the crack opening displacement (COD) func-

tion as the unknown. The substantial effect of the elastic constant ratio G_2/G_1, mode of stresses and geometry conditions of the cracks on dimensionless SIFs have been delineated by means of numerical computation and graphical demonstration. Moreover, the major outcomes of the present analysis can be attributed as follows:

- For $G_2 = 0$ and $G_1 = G_2$, the elementary solution of HSIEs is reduced to two cracks in half plane and infinite plane problems, respectively.
- The equivalence of the stress acting at the crack tip due to the geometric of the cracks resulted in equal values of dimensionless SIFs.
- The value of G_2/G_1, types of stresses and geometry conditions of the crack affect the strength of the materials for two cracks in the upper part of dissimilar materials.

For future developments, the approach used in this paper could be extended to investigate the behavior of dimensionless SIFs for others geometry conditions in dissimilar materials under various mechanical loadings. It also can be extended to the three-dimensional cracks problems in dissimilar materials with guided work from Chen and Lee [27].

Author Contributions: Conceptualization, K.B.H., N.M.A.N.L., N.S. and Z.K.E.; methodology, K.B.H. and N.M.A.N.L.; software, K.B.H. and N.M.A.N.L.; validation, K.B.H. and N.M.A.N.L.; formal analysis, K.B.H. and N.M.A.N.L.; writing—original draft preparation, K.B.H.; writing—review and editing, N.M.A.N.L.; supervision, N.M.A.N.L., N.S. and Z.K.E. All authors have read and agreed to the published version of the manuscript.

Institutional Review Board Statement: Not applicable.

Informed Consent Statement: Not applicable.

Data Availability Statement: Data is contained within the article.

Conflicts of Interest: The authors declare no conflict of interest.

Abbreviations

The following abbreviations are used in this manuscript:

COD	Crack Opening Displacement
CPF	Complex Potentials Function
HSIEs	Hypersingular Integral Equations
MCPs	Modified Complex Potentials
SIFs	Stress Intensity Factors

Glossary of Symbols

The following symbols are used in this manuscript:

$\phi(z), \psi(z), \omega(z)$	Complex Potentials Functions
$\phi_1(z), \psi_1(z), \omega_1(z)$	Upper plane of Complex Potentials Functions
$\phi_{1p}(z), \psi_{1p}(z), \omega_{1p}(z)$	Principal part of Complex Potentials Functions
$\phi_{1c}(z), \psi_{1c}(z), \omega_{1c}(z)$	Complementary part of Complex Potentials Functions
$\phi_2(z), \psi_2(z), \omega_2(z)$	Lower plane of Complex Potentials Functions
$\sigma_x, \sigma_y, \sigma_{xy}$	Stress components
ε	Strain component
G	Shear modulus
v	Poisson's ration
$g(t)$	Crack Opening Displacement function
β_i	Elastic constant

K_{A_j}	Stress Intensity Factors at crack tip A_j
F_{A_j}	Dimensionless Stress Intensity Factors at crack tip A_j
$\displaystyle\fint$	Hypersingular integral and must be defined as a finite part integral
$\simeq$	Similarity equation
$\{N(t_{i0}) + iT(t_{i0})\}_{ij}$	The traction influence on crack i caused by COD function on crack j

References

1. Muskhelishvili, N.I. *Some Basic Problems of the Mathematical Theory of Elasticity*; Noordhoff International Publishing: Leyden, IL, USA, 1953.
2. Gray, L.J.; Martha, L.F.; Ingraffea, A.R. Hypersingular integrals in boundary element fracture analysis. *Int. J. Numer. Methods Eng.* **1990**, *29*, 1135–1158. [CrossRef]
3. Nik Long, N.M.A.; Eshkuvatov, Z.K. Hypersingular integral equation for multiple curved cracks problem in plane elasticity. *Int. J. Solids Struct.* **2009**, *46*, 2611–2617. [CrossRef]
4. Liu, Z.X.; Xu, W.; Yu, Y.; Wu, X.R. Weight Functions and Stress Intensity Factors for Two Unequal-Length Collinear Cracks in an Infinite Sheet. *Eng. Fract. Mech.* **2019**, *209*, 173–186. [CrossRef]
5. Lai, J.; Schijve, J. The stress intensity factor and stress concentration for a finite plate with a single crack emanating from a hole. *Eng. Fract. Mech.* **1990**, *36*, 619–630. [CrossRef]
6. Zhang, J.; Qu, Z.; Liu, W.; Wang, L. Automated numerical simulation of the propagation of multiple cracks in a finite plane using the distributed dislocation method. *Comptes Rendus Mec.* **2019**, *347*, 191–206. [CrossRef]
7. Legros, B.; Mogilevskaya, S.G.; Crouch, S.L. A boundary integral method for multiple circular inclusions in an elastic half-plane. *Eng. Anal. Bound. Elem.* **2004**, *28*, 1083–1098. [CrossRef]
8. Liu, X.; Guo, J. Interaction between a screw dislocation and oblique edge crack in a half-infinite MEE solid. *Theor. Appl. Fract. Mech.* **2016**, *86*, 225–232. [CrossRef]
9. Elfakhakhre, N.R.F.; Nik Long, N.M.A.; Eshkuvatov, Z.K. Numerical solutions for cracks in an elastic half-plane. *Acta Mech. Sin.* **2019**, *35*, 212–227. [CrossRef]
10. Chen, Y.Z. Multiple crack problems for two bonded half planes in plane and antiplane elasticity. *Eng. Fract. Mech.* **1986**, *25*, 1–9. [CrossRef]
11. Chen, Y.Z.; Hasebe, N. Stress-intensity factors for curved circular crack in bonded dissimilar materials. *Theor. Appl. Fract. Mech.* **1992**, *17*, 189–196. [CrossRef]
12. Isida, M.; Noguchi, H. Arbitrary array of cracks in bonded half planes subjected to various loadings. *Eng. Fract. Mech.* **1993**, *46*, 365–380. [CrossRef]
13. Zhou, Y.T.; Li, X.; Yu, D.H. Integral method for contact problem of bonded plane material with arbitrary cracks. *Comput. Model. Eng. Sci* **2008**, *36*, 147–172.
14. Long, G.; Xu, G. A combined boundary integral method for analysis of crack problems in multilayered elastic media. *Int. J. Appl. Mech.* **2016**, *8*, 1650070. [CrossRef]
15. Hamzah, K.B.; Nik Long, N.M.A.; Senu, N.; Eshkuvatov, Z.K. Stress intensity factor for multiple cracks in bonded dissimilar materials using hypersingular integral equations. *Appl. Math. Model.* **2019**, *73*, 95–108. [CrossRef]
16. Hamzah, K.B.; Nik Long, N.M.A.; Senu, N.; Eshkuvatov, Z.K. Stress intensity factor for bonded dissimilar materials weakened by multiple cracks. *Appl. Math. Model.* **2020**, *77*, 585–601. [CrossRef]
17. Hamzah, K.B.; Nik Long, N.M.A.; Senu, N.; Eshkuvatov, Z.K.; Ilias, M.R. Stress intensity factors for a crack in bonded dissimilar materials subjected to various stresses. *Univers. J. Mech. Eng.* **2019**, *7*, 179–189. [CrossRef]
18. Chen, Y.Z.; Lin, X.Y.; Wang, X.Z. Numerical solution for curved crack problem in elastic half-plane using hypersingular integral equation. *Philos. Mag.* **2009**, *89*, 2239–2253. [CrossRef]
19. Monegato, G. Numerical evaluation of hypersingular integrals. *J. Comput. Appl. Math.* **1994**, *50*, 9–31. [CrossRef]
20. Mayrhofer, K.; Fischer, F.D. Derivation of a new analytical solution for a general two-dimensional finite-part integral applicable in fracture mechanics. *Int. J. Numer. Method Eng.* **1992**, *33*, 1027–1047. [CrossRef]
21. Mason, T.C.; Handscomb, D.C. *Chebyshev Polynomials*; Chapman and Hall/CRC: Boca Raton, FL, USA. 2003.
22. Kythe, P.K.; Schaferkotter, M.R. *Handbook of Computational Methods for Integration*; Chapman and Hall/CRC: Boca Raton, FL, USA, 2004.
23. Petersen, R.C. Accurate critical stress intensity factor Griffith crack theory measurements by numerical techniques. *SAMPE J. Soc. Adv. Mater. Process. Eng.* **2013**, *2013*, 737–752.
24. Wang, T.C. Fundamentals of interface mechanics. *Ref. Modul. Mater. Sci. Mater. Eng.* **2003**, *8*, 89–135.
25. Choi, H.J. Thermoelastic interaction of two offset interfacial cracks in bonded dissimilar half-planes with a functionally graded interlayer. *Acta Mech.* **2014**, *225*, 2111–2131. [CrossRef]
26. Chen, Y.Z.; Hasebe, N. Fredholm integral equation for the multiple circular arc crack problem in plane elasticity. *Arch. Appl. Mech.* **1997**, *67*, 433–446. [CrossRef]
27. Chen, Y.Z.; Lee, K.Y. Numerical solution of three-dimensional crack problem by using hypersingular integral equation. *Comput. Methods Appl. Mech. Eng.* **2001**, *190*, 4019–4026. [CrossRef]